

Hybrid materials doped with lithium ions

ELŻBIETA ŻELAZOWSKA^{1*}, EWA RYSIAKIEWICZ-PASEK²

¹Institute of Glass, Ceramics, Refractory and Construction Materials – The Glass Branch in Cracow, ul. Lipowa 3, 30-702 Kraków, Poland

²Institute of Physics, Wrocław University of Technology, Wybrzeże Wyspiańskiego 27, 50-370 Wrocław, Poland

*Corresponding author: ezelazowska@isic.krakow.pl

Sol–gel derived lithium-ion conducting organic–inorganic hybrid materials have been synthesized from tetraethyl orthosilicate (TEOS), propylene glycol, ethylene glycol dimethacrylate, poly(vinyl alcohol), vinyl acetate, ethyl acetoacetate, poly(methyl methacrylate), propylene carbonate and some other precursors and solvents. The mass fraction of the organic additions in the gels and the level of the lithium salt doping (LiClO_4) were ~ 40 mass% and 0.01%, respectively. The morphological and structural properties of the gels were investigated by a scanning electron microscope equipped with energy dispersive X-ray spectroscopy (SEM/EDX), X-ray diffraction (XRD), and Fourier-transform infrared spectroscopy (FTIR) and ^{29}Si MAS Nuclear Magnetic Resonance (^{29}Si MAS NMR). The hybrid gels obtained were amorphous and colourless transparent or slightly opalescent, with the room temperature ionic conductivities of the order of 10^{-3} Scm^{-1} . The results of FTIR spectroscopy and ^{29}Si MAS NMR investigations have revealed strong influence of the organic modification, resulting in the direct chemical bonding between organic and inorganic components of the gels. The WO_3 -based electrochromic cells with the hybrids obtained being applied as the electrolytes were able to be reversibly coloured and bleached in the optical transmittance range of $\sim 58\%$ to 5% at around 550 nm.

Keywords: organic–inorganic hybrids, sol–gel, lithium electrolyte, ionic conductivity.

1. Introduction

Solid materials with relatively high ionic conductivities at ambient temperatures have potentially a wide range of practical applications in the solid-state rechargeable batteries [1] and advanced electrochemical devices, such as electrochromic displays, variable reflectance mirrors or smart windows [2, 3]. In the last years, intensive development has been observed in the use of sol–gel process for preparing the organically modified silanes (ormosils) [4, 5]. Amorphous organic–inorganic hybrid materials, which are synthesized through relatively easy and low cost sol–gel route and have the potential of being used in integrated optics and solid electrolyte (ormolyte) applications have recently attracted a great deal of research attention [6, 7].

Many organic compounds have been proposed as components of the sol–gel derived hybrid electrolytes, including polyacrylonitrile (PAN), poly(ethylene oxide)

(PEO), poly(tetramethylene oxide) (PTMO), poly(methyl methacrylate) (PMMA), polyethylene glycol (PEG), polypropylene glycol (PPG), poly(vinylidene fluoride) (PVDF), some network polymers prepared by cross-linking reactions, and mixtures of polymers from these two groups [8–11].

Among the possible organic additions, polyether polymers have been studied extensively due to their favourable feature of being miscible with many kinds of liquid electrolytes for lithium batteries, [9] and [12]. CHAKER *et al.* [7] have reported on siloxane-poly-(propylene oxide) (PPO, with 2000 and 4000 g/mol molecular weight) based hybrid electrolytes doped with sodium perchlorate (NaClO_4), obtained by the sol–gel method and exhibiting the ionic conductivity of $8.9 \times 10^{-4} \text{ S cm}^{-1}$ at room temperature. DAHMOUCHE *et al.* [13] and DE SOUZA *et al.* [14] have investigated lithium ion-conducting ormolytes with ionic conductivities higher than 10^{-4} S m^{-1} at room temperature. They have found that in the hybrids prepared by sol–gel process from the mixture of tetraethyl orthosilicate (TEOS), polyethylene glycol (PEG), and lithium salt (LiClO_4), the organic and inorganic parts were not chemically bonded, while the chemical bonding has been revealed in the hybrid electrolytes obtained from a mixture of 3-isocyanatopropyltriethoxysilane, O,O'-bis-(2-aminopropyl)-polyethylene glycol or O,O'-bis-(2-aminopropyl)-polypropylene glycol, and lithium salt.

Due to appropriate doping and controlling of a molecular structure by organic modification to enable fast proton and/or lithium ion conduction, organic–inorganic hybrid materials have proved to be a remarkable family of amorphous solid state electrolytes for promising practical applications. On the other hand, the ionic conductivity of the hybrid electrolytes has been found to be strongly dependent on the morphology and microstructure [9, 15, 16].

2. Experiment

2.1. Materials for hybrid synthesis

The hybrid materials for electrolytes have been synthesized from the tetraethyl orthosilicate (TEOS, $[\text{Si}(\text{OC}_2\text{H}_5)_4]$), propylene glycol (propane-1,2-diol; PG), ethylene glycol dimethacrylate ($\text{C}_{10}\text{H}_{14}\text{O}_4$, EGDMA), poly(vinyl alcohol) (ethanol,

T a b l e 1. Components of the starting solutions.

Sample	Components	Lithium salt/solvent/ fraction	Appearance, remarks
A	TEOS, PG, VAM, PMMA, PC, CH_2Cl_2 , ethanol	LiClO_4 /ethanol/0.01	colourless, transparent
B	TEOS, PG, EGDMA, PVA, PMMA VAM, EAA, CH_2Cl_2 , methanol, ethanol	LiClO_4 /ethanol//0.01	colourless, slightly opalescent
C	TEOS, PG, PVA, VAM, EGDMA, PC, methanol, ethanol	LiClO_4 /PC/0.01	colourless, transparent

PVA, $M_w \approx 72000$), vinyl acetate (ethenyl acetate; VAM), ethyl acetoacetate (ethyl 3-oxobutanoate; EAA), poly(methyl methacrylate) (poly(methyl 2-methylpropenoate), PMMA, $M_w \approx 120000$), propylene carbonate (4-methyl-1,3-dioxolan-2-one, $C_4H_6O_3$, PC), dichloromethane (CH_2Cl_2), ethanol and methanol, precursors and solvents. Components (at least of reagent grade, Merck and Aldrich) of the starting solutions for hybrids under investigation are listed in Tab. 1.

Mass fractions of the organic compounds were calculated on ~40 mass% in the gels. The level of the lithium salt doping ($LiClO_4$ in solution with PC or ethanol) was ~0.01 for all the gels synthesized.

2.2. Experimental procedure

2.2.1. Sol–gel procedure

Silica components of the gels under investigation were prepared by mixing TEOS [$Si(OC_2H_5)_4$] (0.09 mol for each hybrid gel) and distilled water with the stoichiometric molar ratio of $TEOS:H_2O = 1:4$. As a catalyst, 36.6% HCl was added drop by drop, up to $pH = 2$. Solutions of PMMA or PVA (1.5 g and/or 1 g, respectively) in organic solvents (dichloromethane, methanol and ethanol) were prepared under stirring for at least 3 h at a temperature of 45 ± 5 °C. Solutions of TEOS, after stirring for 1 h, were mixed with solutions of the PMMA or PVA. Then, under the continuous stirring, PG and VAM (6 ml and 15 ml, respectively) per each gel and the other organic compounds (0.08 mol of EGDMA, and/or PC and EAA in the weigh amounts equal to that of VAM addition) were added one by one. The resulting mixtures after being stirred for ~1 h were poured into the plastic dishes. The gelation process occurred within several hours to 1 day. The hybrid gels were aged at ambient temperature for 2 weeks and then heated in an electric oven for 3 h at a temperature of 105 °C.

2.2.2. Spray pyrolysis coating procedure for thin metal oxide electrochromic electrodes

The spectral and current–voltage characteristics have been obtained for a $WO_3-V_2O_5$ thin film electrochromic system. The layers of the sol–gel derived lithium ion doped organic–inorganic hybrid materials under investigation were applied as the solid electrolytes with the aim to determine their potential to be useful for room-temperature electrochemical applications. Electrochromic devices consisted of: a transparent conducting layer ($SnO_2:F$)/a cathodic, active electrochromic layer (WO_3)/an ion conducting layer (hybrid electrolyte)/an anodic counter electrode layer (NiO)/a transparent conducting layer ($SnO_2:F$), which were prepared for this study as the symmetric multilayer structures of a smart window arrangement.

Thin electrochromic films of tungsten oxide and vanadium oxide for an active and a counter electrode, respectively, were obtained by a spray pyrolysis method, at the substrate temperature of about 680 °C and 670 °C, respectively. The transparent electrode substrates were soda-lime glass plates ($25 \times 50 \times 4$ mm³) coated with fluorine doped tin oxide ($SnO_2:F$, K-Glass, Pilkington). The substrates to be coated were carefully washed with a detergent solution, etched in a 4% aqueous solution of hydrofluoric acid for 5 min, and then rinsed with distilled water and ethanol.

Tungsten (VI) oxide acetylacetonate $\text{WO(VI)(C}_5\text{H}_7\text{O}_2)_4$ and vanadyl acetylacetonate ($\text{VO(IV)(C}_5\text{H}_7\text{O}_2)_2$, bis(2,4-pentanedionato)vanadium(IV) oxide) in solution with dichloromethane, were used as precursors of the metal oxide electrochromic films. Detailed procedures were used for thin metal oxide films and preparation of electrochromic cells followed that described in [17]. The thickness of the films obtained when measured with a “Talystep” microprofilometer (Rank Taylor Hobson Ltd., Great Britain), was about 120 nm and 150 nm for WO_3 and V_2O_5 , respectively.

2.3. Instruments and measurements

The obtained hybrid materials and metal oxide films were characterized for morphology by scanning electron microscopy equipped with energy dispersive X-ray spectroscopy (SEM/EDX, JEOL JSM 5400 with LINK An 10/5, NOVA NANOSEM-FEI). Fourier transform infrared spectroscopy (Bio-Rad FTS-60VM FTIR spectrometer, KBr technique), nuclear magnetic resonance ^{29}Si MAS NMR (NMR spectrometer at the magnetic field 7.05 T) and X-ray diffraction (XRD 7, Seifert diffractometer) were used for examination of microstructure of the hybrids obtained in this work. Spectral characteristics of the WO_3 -based thin film electrochromic cells under investigation in the coloured and bleached states have been obtained by applying a DC voltage of $\pm(1.4\text{--}1.8)$ V between a $\text{WO}_3/\text{SnO}_2\text{:F}$ active electrode and a $\text{V}_2\text{O}_5/\text{SnO}_2\text{:F}$ counter electrode, being registered with a Jasco V-570 spectrophotometer. The spectral and current–voltage characteristics of the electrochromic cells with hybrid electrolytes were observed at \pm polarized DC potential of $\pm(1.4\text{--}3.5)$ V applied through a laboratory-made potentiostat/galvanostat. The AC conductivity measurements were performed by using an Alpha N dielectric analyser (Novocontrol) in the frequency range of 7.32×10^{-2} Hz– 3×10^6 Hz at room temperature. The measurements were carried out in the specially constructed sample cells with the platinum plate electrodes pressed against the sample surface. The area of the contact was about 0.5 cm^2 .

3. Results and discussion

3.1. Structural characterization

3.1.1. XRD and SEM/EDX results

The appearance of the gels after heat treatment is described in Tab. 1. All the gels obtained have revealed an amorphous structure under XRD examination. The XRD pattern, typical of hybrids under investigation, is shown in Fig. 1.

Typical SEM images (surface view and fractured surface, at a magnification of $50000\times$) of the WO_3 , V_2O_5 thin films obtained in this work for the electrochromic electrodes and of the hybrids A, B and C applied as electrolytes in the electrochromic cells of the $\text{WO}_3\text{--V}_2\text{O}_5$ system are shown in Figs. 2a–2c and 2d–2f, respectively.

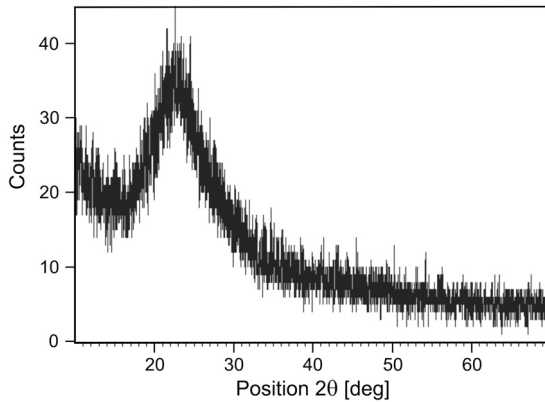


Fig. 1. XRD pattern of the hybrid A, typical of the hybrids under investigation.

The EDX results typical of the organic–inorganic hybrid gels under investigation (for gel C, synthesized from: TEOS, PG, PVA, VAM, EGDMA, PC, LiClO_4 , methanol, ethanol) are presented in Fig. 3.

The scanning electron microscopy coupled with X-ray energy dispersive spectroscopy (SEM/EDX) in agreement with the XRD investigation results have revealed the obtained metal oxide films to be porous and polycrystalline with uniformly distributed nano-sized crystallites. The amorphous and significantly porous morphology has been observed for the sol–gel derived hybrid electrolytes A, B and

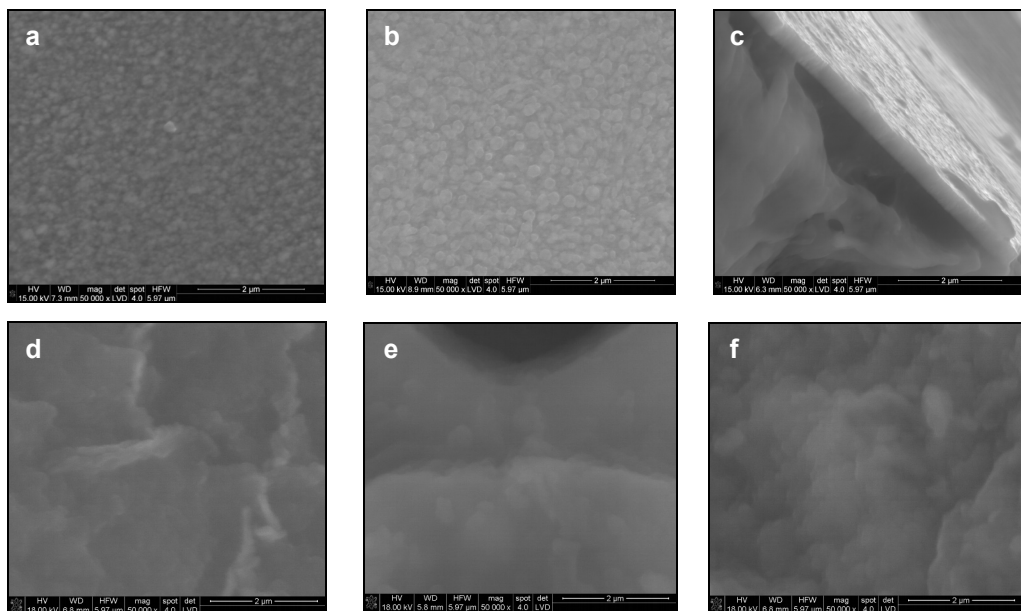


Fig. 2. SEM images of thin films of WO_3 (a), V_2O_5 (b – surface view, c – fractured surface) and hybrid gels: A (d), B (e), C (f), at a magnification of 50000 \times .

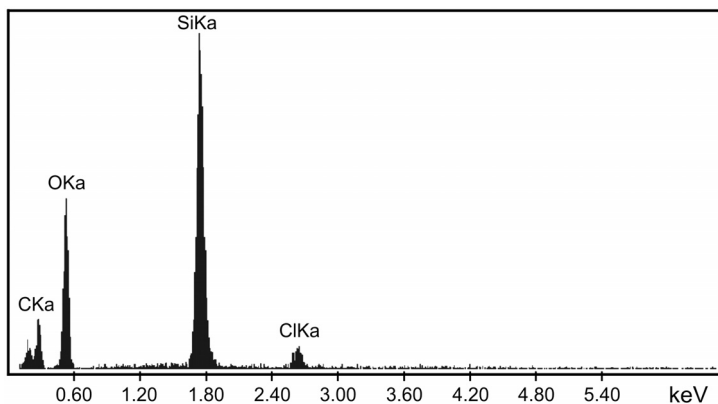


Fig. 3. EDX spectrum of a micro-area surface registered at a magnification of 5000 \times for hybrid gel C synthesized from TEOS, PG, EGDMA, PVA ($M_w \approx 72000$), VAM, PC, LiClO₄ and organic solvents.

especially C (Figs. 2d–2f, respectively) and such a thin microstructure can be seen as advantageously available for a diffusion of alkali ions.

3.1.2. ²⁹Si MAS NMR and FTIR spectroscopy results

²⁹Si MAS NMR spectra and calculated results of the hybrid gels after heat treatment at 105 °C are shown in Fig. 4 and Tab. 2, respectively.

²⁹Si MAS NMR spectra of the hybrid electrolytes exhibit peak profiles with different amounts of the Q₄, Q₃ and Q₂ structural units corresponding to the silicon Si in coordination of 4, 3 or 2 in respect to the bridging oxygen atoms. The analysis of these spectra was based on the numerical values of the parameter A1 equal to the ratio of Q₄/Q₃ and parameter A2 equal to the ratio of Q₄/Q₂ calculated from the relative fractions of the peak area, corresponding to the appropriate Q species, where Q₄ value

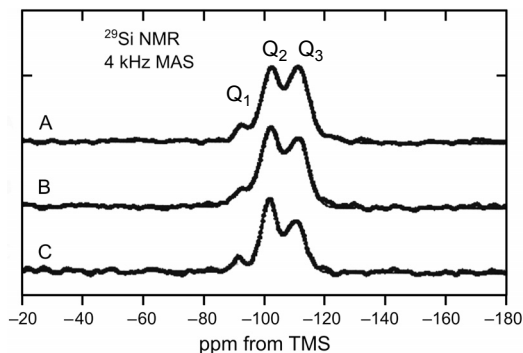


Fig. 4. ²⁹Si MAS NMR spectra for organic–inorganic hybrid electrolytes under investigation A, B and C (the Q₄, Q₃ and Q₂ peaks are corresponding to the structural units corresponding to the silicon Si in coordination 4, 3 or 2).

Table 2. Isotropic chemical shifts (δ , ppm), line widths (half width at half maximum (hwhm), ppm) and relative fraction (%) of Q_n units in the hybrid materials.

Sample	Q_2		Q_3		Q_4		A1 = $\frac{Q_4}{Q_3}$	A2 = $\frac{Q_4}{Q_2}$
	$-\delta$, hwhm [ppm]; relative share [%]		$-\delta$, hwhm [ppm]; relative share [%]		$-\delta$, hwhm [ppm]; relative share [%]			
A	-92.4 (5.7)	7	-101.6 (7.1)	40	-110.8 (8.5)	50	1.25	7.14
B	-93.0 (9.0)	12	-101.7 (7.0)	41	-110.8 (8.6)	47	1.15	3.92
C	-91.7 (5.5)	8	-101.5 (6.2)	48	-110.3 (7.9)	44	0.92	5.50

at approximately -109 ppm corresponds to $[\text{SiO}_4]$ tetrahedrons. The higher the A1 and A2 values, the higher the poly-condensation degree of the silicon-oxygen network. The observed chemical shifts were referenced to the signal of tetramethyl silane (TMS).

The NMR measurements (Tab. 2), with a good agreement with results of SEM/EDX, indicated the poly-condensation of the inorganic network to be relatively less developed for hybrids B and C, with the (PG, EGDMA, PVA, PMMA, VAM, EAA) or (PG, PVA, VAM, EGDMA, PC) organic additives, respectively, than that of hybrid A, prepared with organic part containing PG, VAM, PMMA and PC. Additionally, the time of gelation as short as about 5–6 h and an enormous increase in the viscosity of the gels, especially just before the end of gelation process were observed for all the hybrids under investigation. A similar effect was reported by BOONSTRA *et al.* [18], among others, and it can be ascribed to the poly-condensation of inorganic structural units overlapped with cross-linking process. The course of condensation, as observed for all the hybrid gels under investigation, seems to be associated with cross-linking polymerization of the organic and inorganic groups connected with formation of the cross-linked chains of particles, especially due to the presence of the carboxylic groups originated from acrylic acid derivatives. The cross-linking effect of the carboxylic groups on a surface polymerization and grown of the primary created particles has already been reported [19, 20].

FTIR spectra of the sol–gel derived hybrids obtained in this work are shown in Fig. 5.

In the FTIR spectra of the sol–gel derived hybrid gels synthesized in this work and investigated after the heat treatment at a temperature of 105 °C, the observed broad absorption bands at around 3456 – 3435 cm^{-1} are assigned to stretching vibrations of OH^- groups originated from residual water and those from the organic components (PVA, VAM) [23, 24]. The situation of these bands corresponds to differing organic additions in the hybrids. Additionally, in the IR spectra of the gels before the heat treatment, residual absorption signals from asymmetric stretching vibrations ν_{as} of the CH_2 groups and C-H_x bonds of aliphatic organic groups, were observed in a range of about 2980 – 2880 cm^{-1} [5, 23].

The disappearance of signals from these groups as well as those at around 1460 – 1390 cm^{-1} corresponding to vibrations of the bonds in organic parts

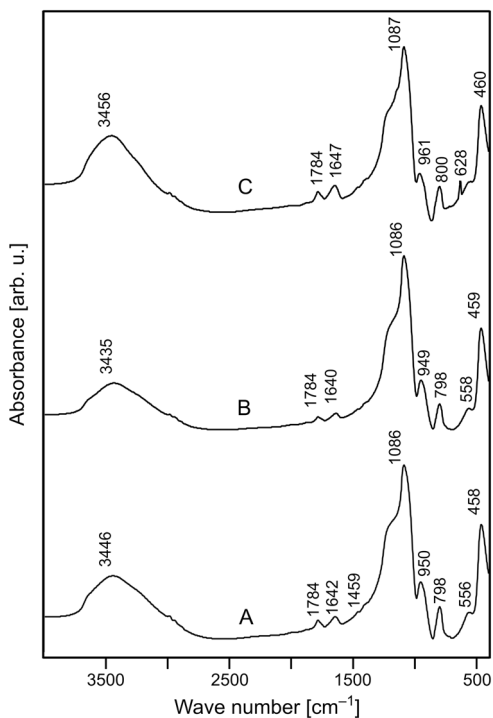


Fig. 5. FTIR spectra of hybrid gels A, B and C, heated at a temperature of 105 °C.

(COH- deformation, $\nu_s(-\text{COO}^-)$, $\delta_{\text{as}}(\text{CH}_3)$ groups) after heating at 105 °C, can be ascribed to the incorporation of the organics, resulting in organic–inorganic bonding and formation of a hybrid structure of the gels.

The bands located at around 1640 cm^{-1} are characteristic of adsorbed water (H–O–H), while those at around 1784 cm^{-1} correspond to the stretching vibrations of the C=O bonds and can be assigned to the etheric oxygen groups –C(=)–O– originated from the carboxylic acid derivative (PMMA) and/or from acetic acid esters (VAM, EAA) [11, 23]. In the case of hybrids under investigation, the absorption bands related to C=O double bond vibrations are relatively weak. It can be supposed that in all the hybrids obtained, and especially, gels A and B, there have occurred both the organic–inorganic polymerization and a cross-linking process [19].

Three fundamental bands of the origin of Si–O vibrations, at about 1090 cm^{-1} (1087 cm^{-1} for gel C and 1086 cm^{-1} for gels A and B), 800 cm^{-1} and 460 cm^{-1} were found in the FTIR spectra of all the gels under investigation. The first two correspond to asymmetric and symmetric Si–O stretching vibrations, respectively, and the last one to the O–Si–O bending vibrations. The presence of these bands, and especially the bands at about 800 cm^{-1} , is the evidence of a considerable degree of polymerization of the silica fragments into network due to the formation of oxygen bridges between SiO_4 tetrahedrons. The large absorption band in a range of 1250 cm^{-1} –1000 cm^{-1} with the dominating vibration mode at about 1087 cm^{-1} (ν_{as} Si–O) seems to be overlapping other vibration modes. A shoulder on the dominating vibration mode at around

1200 cm^{-1} can be assigned to the C–O stretching vibration and there in a region at around $1110\text{--}1000\text{ cm}^{-1}$ the vibrations from Si–O–C can be overlapped [21, 24].

The absorption band for C–O bonds overlapped with Si–O vibrations band without splitting the main absorption band at around 1087 cm^{-1} can be ascribed to the conversion of the C–OH bonds in PVA and VAM to C–O–Si bonds, responsible for the cross-linking of the organic parts to silica and due to a hybrid structure of the gels [4].

Besides these bands, in the spectra of the gels under investigation, the absorption peaks located at around 950 cm^{-1} correspond to ν_{as} Si–OH stretching vibrations [21, 22]. Additionally, in the region at around 960 cm^{-1} the absorption corresponding to the vibrations of the hydrogen bonding ($\delta(\text{COH})$) can overlap that of the stretching vibrations of the non-bridging oxygen atoms, *e.g.*, Si–OH [23].

The relatively weak bands at around $556\text{--}558\text{ cm}^{-1}$ corresponding to absorption of lithium in LiClO_4 and bonded to organics, are observed in the FTIR spectra of all the hybrid electrolytes obtained [23]. Additionally, in the spectrum of hybrid electrolyte C, besides the lithium bonded to organics, the peak from ClO_4^- at 628 cm^{-1} can be observed, indicating the presence of the free lithium ions [25].

The FTIR data are in a good agreement with SEM/EDX and ^{29}Si MAS NMR data, and from this it was concluded that the degree of the inorganic poly-condensation in the gel A is higher than that of the gel B, and especially, gel C.

3.2. Electrochemical evaluation

3.2.1. AC conductivity and cycling voltammetry

Figure 6 shows room temperature conductivities of hybrids A and C as a function of frequency ranging from about $7.32 \times 10^{-2}\text{ Hz}$ to $3 \times 10^6\text{ Hz}$.

AC conductivities of the order of 10^{-3} S cm^{-1} , when measured at room temperature have been typical values of the hybrid electrolytes investigated.

The conductivities of hybrids A and B proved to have almost the same dependence of conductivity on the frequency. The best value of ionic conductivity of about $6.8 \times 10^{-3}\text{ S cm}^{-1}$ was noticed for the hybrid electrolyte C, with ethylene glycol

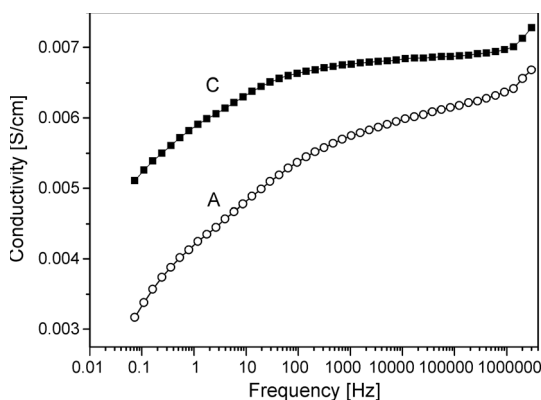


Fig. 6. Conductivities of hybrids A and C as a function of frequency at room temperature.

dimethacrylate (EGDMA), polyvinyl alcohol (PVA), vinyl acetate (VAM), and propylene carbonate (PC) organic additives used as the gel precursors. The conductivities of hybrids A and B, which were prepared with addition of PMMA, propylene glycol (PG) and VAM, have proved to be a little lower than that of hybrid C and almost equal to each other, although these gels differ in the content of such organic additives as PG, EGDMA, PVA or EAA. The main difference in composition of the hybrids under investigation is the content of PMMA in gels A and B, when the acrylic acid derivatives are known for their cross-linking ability [20, 26]. On the other hand, it is well known that the cross-linking density affects the flexibility of the polymer matrix: the lower the cross-linking density, the more flexible the polymer matrix becomes [27]. The decrease in ionic conductivity with an increase of the content of polymer additives in the gel matrix is related to the increase in the cross-linking density, resulting in a decrease of the flexibility of the hybrid matrix, and consequently, the mobility of ionic charge carriers decreases.

Apart from the high conductivity, electrochemical stability is an important characteristic of electrolytes for recent advanced applications. All the organic–inorganic hybrid materials obtained in this work were examined as electrolytes for the symmetric electrochemical cells of $\text{WO}_3\text{--V}_2\text{O}_5$ thin film system with an electrochromic window arrangement.

The cyclic voltammetry (CV) results obtained for an electrochromic cell of the $\text{WO}_3\text{--V}_2\text{O}_5$ thin film system with hybrid electrolyte B under a potential signal of a rectangular shape applied by means of a potentiostat-galvanostat, typical of the materials under investigation, are shown in Fig. 7.

The cyclic voltammogram presented in Fig. 7b was recorded at a sweep rate of 50 mV/s and with potentials ranging from -3.0 to 3.0 V after about 10^3 colouring–bleaching cycles.

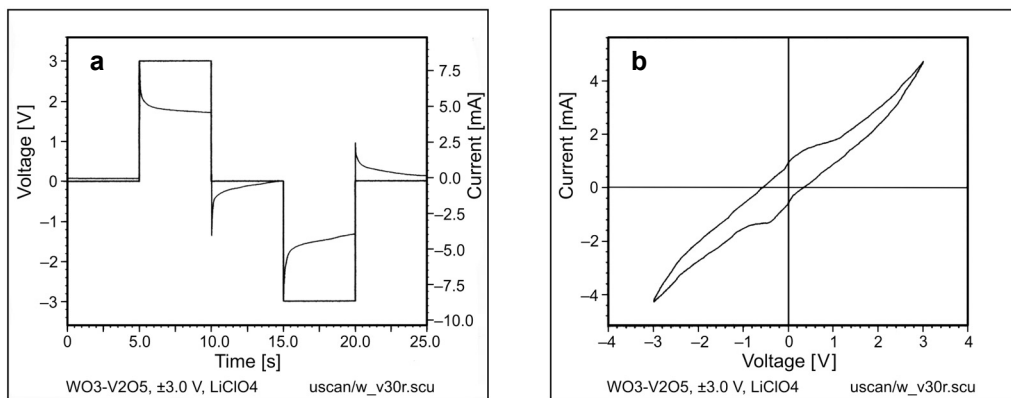


Fig. 7. Typical current response (a) and cyclic voltammogram (b) for thin film tungsten oxide–vanadium oxide electrochromic cell with organic–inorganic hybrid electrolyte B, cycled at a voltage of ± 3.0 V (cycled area: 4 cm^2 ; scan rate 50 mV/s).

The CV course has been observed to stay established after a few initial cycles. The electrochromic films exhibit two distinct reduction-oxidation peaks at the low voltage values, which may be associated with redox couple in the V_2O_5 film and two weakly distinguishable peaks which can be attributed to lithium ions intercalation/deintercalation in the WO_3 film. The shape of the CV curve is typical of the diffusion controlled and a highly reversible lithium intercalation/deintercalation process and well corresponds to the symmetric current response of the cell (Fig. 7a), indicating hybrid materials under investigation to be a sufficient host for reversible intercalation/deintercalation of lithium ions. On the other hand, the colouring–bleaching cycles of the WO_3 film have been performed very fast and associated with sharp colour changes. Such a behaviour of the WO_3 film seems to be attributed to the nano-sized polycrystalline morphology to be favourable to the colouring efficiency enhancement due to the probable participation of the surface and pore bonded protons.

3.2.2. Transmission characteristics

Figure 8 shows typical UV/VIS/NIR spectral transmittance characteristics of a WO_3 – V_2O_5 symmetric thin film electrochromic system of an electrochromic window arrangement with a WO_3 layer for the active electrode and a V_2O_5 layer for the complementary counter electrode. Electrochromic layers were coated onto glass with the electro-conductive films of fluorine (F) doped SnO_2 , and laminated with hybrid C employed as an electrolyte.

The spectral measurements conducted after up to 30 colouring–bleaching cycles were performed at potential values ranging from ± 1.4 to ± 1.8 V. The presented data

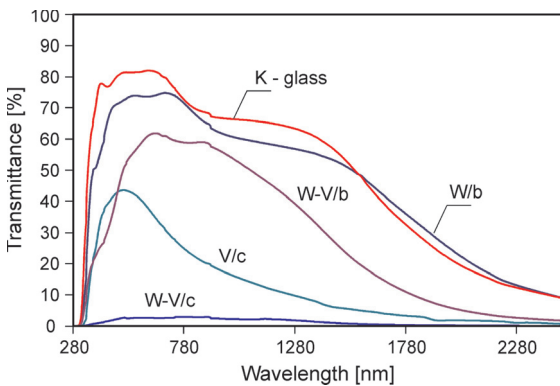
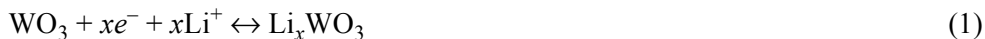


Fig. 8. Typical spectral transmittance characteristics for a WO_3 – V_2O_5 thin film system of an electrochromic window arrangement, coloured and bleached under ± 1.8 V polarized DC voltage, with a layer of hybrid gel as electrolyte (C: synthesized from TEOS, PG, PVA, PC, VAM, EGDMA, $LiClO_4$, dichloromethane and ethanol, precursors and solvents). The electrochromic layers are coated onto the sheets of glass with electro-conductive transparent electrodes ($SnO_2:F$); the labels W, V, W–V, correspond to the electrodes of WO_3 , V_2O_5 and WO_3 – V_2O_5 cell in a bleached (b) and coloured state (c), respectively.

were obtained both in the coloured and bleached states under a ± 1.8 V polarized DC voltage.

The thin film coating structure of the electrochemical cell used for CV and spectral transmittance examination corresponds to a system in which lithium ions are intercalated and deintercalated in tungsten oxide and vanadium oxide layers according to the electrochemical reactions (1) and (2), respectively:



The vanadium pentoxide displays both cathodic and anodic colouration, but it is applied mainly for ion storage counter electrodes because of a change in optical spectrum not as large as that of the WO_3 [28]. In a bleached state the amorphous V_2O_5 layer is yellow and after lithium insertion it becomes blue-green due to the absorption band at around 450 nm, typical of intervalence transfers between V^{4+} and V^{5+} [29]. In crystalline V_2O_5 the insertion of Li^+ follows the reaction (2) and results in a colour change from yellow to blue (Fig. 8, V/c) [30].

In the electrochromic systems under investigation, the insertion of lithium ions changes the transmission in the visible range (at a wavelength of 550 nm) from about 58% to about 5% or 40% when the WO_3 and V_2O_5 electrochromic electrodes are in a coloured state, respectively (Fig. 8). All the hybrid gels obtained in this work, when applied as the electrolytes in a WO_3 – V_2O_5 electrochromic system have proved to be able to be reversibly coloured and bleached in a short time of less than 2 s and with significant changes in the optical transmittance, with modulation from about 60% to 5%.

The transmittance characteristics in the VIS/NIR spectral range presented in Fig. 8, in a good agreement with the SEM observations have proved to be characteristic of polycrystalline non-stoichiometric thin films of tungsten oxide and vanadium pentoxide with spectral reflective properties connected with Drude's free-electron modulation in NIR in a bleached and coloured state, respectively [31, 32].

4. Conclusions

Sol–gel derived, amorphous Li-ion conductive organic–inorganic hybrid materials with the ionic conductivities of about $(6.2\text{--}6.8)\times 10^{-3}$ S cm^{-1} at room temperature and containing $\sim 40\%$ of the organic additives were obtained using tetraethyl orthosilicate TEOS, propylene glycol, ethylene glycol dimethacrylate, poly(vinyl alcohol), vinyl acetate, ethyl acetoacetate, poly(methyl methacrylate), propylene carbonate, lithium perchlorate and organic solvents. Direct chemical bonding between the inorganic and organic parts have been revealed from FTIR and ^{29}Si MAS NMR spectra. The polycondensation process overlapped with cross-linking polymerization has been observed, especially in the hybrids containing PMMA. The room temperature

conductivity of all the hybrids under investigation is almost linear in the frequency range of about 50 Hz to 3.5×10^5 Hz. The symmetric situation and shape of cathodic and anodic peaks for active- and counter-electrode due to ion intercalation and deintercalation, respectively, indicate materials under investigation to be kinetically favoured insertion hosts. On the other hand, relatively sharp peaks at the highest values of the voltage applied makes the association of lithium and proton conductance possible, due to protons bonded with surface pores of the nano-sized polycrystalline structure of the hybrids. All the hybrid materials obtained in this work have proved to be electrochemically effective in reversible electrochromic reactions depending on reversible intercalation–deintercalation of the lithium ions, which makes them prospective as electrolytes for ambient temperature electrochemical and optoelectronic applications.

References

- [1] KONO M., HAYASHI E., NISHIURA M., WATANABE M., *Chemical and electrochemical characterization of polymer gel electrolytes based on poly(alkylene oxide) macromonomer for application to lithium batteries*, Journal of The Electrochemical Society **147**(7), 2000, pp. 2517–2524.
- [2] GLÄSER H.J., *Large Area Glass Coating*, Von Ardenne Anlagentechnik GMBH, Dresden 2000, pp. 377–393.
- [3] GRANQVIST C.G., AVENDAÑO E., AZENS A., *Electrochromic coatings and devices: survey of some recent advances*, Thin Solid Films **442**(1–2), 2003, pp. 201–211.
- [4] PEREIRA A.P.V., VASCONCELOS W.L., ORÉFICE R.L., *Novel multicomponent silicate–poly(vinyl alcohol) hybrids with controlled reactivity*, Journal of Non-Crystalline Solids **273**(1–3), 2000, pp. 180–185.
- [5] JITIANU A., BRITCHI A., DELEANU C., BADESCU V., ZAHARESCU M., *Comparative study of the sol–gel processes starting with different substituted Si-alkoxides*, Journal of Non-Crystalline Solids **319**(3), 2003, pp. 263–279.
- [6] ATKINS G.R., KROLIKOWSKA R.M., SAMOC A., *Optical properties of an ormosil system comprising methyl- and phenyl- substituted silica*, Journal of Non-Crystalline Solids **265**(3), 2000, pp. 210–220.
- [7] CHAKER J.A., DAHMOUCHE K., SANTILLI C.V., PULCINELLI S.H., BRIOIS V., FLANK A.-M., JUDENSTEIN P., *Siloxane-polypropyleneoxide hybrid ormolytes: structure-ionic conductivity relationships*, Journal of Non-Crystalline Solids **304**(1–3), 2002, pp. 109–115.
- [8] KONO M., HAYASHI E., WATANABE M., *Preparation, mechanical properties, and electrochemical characterization of polymer gel electrolytes prepared from poly(alkylene oxide) macromonomers*, Journal of The Electrochemical Society **146**(5), 1999, pp.1626–1632.
- [9] NAKAJIMA H., NOMURA S., SUGIMOTO T., NISHIKAWA S., HONMA I., *High temperature proton conducting organic/inorganic nanohybrids for polymer electrolyte membrane*, Journal of The Electrochemical Society **149**(8), 2002, pp. A953–A959.
- [10] SONG J.Y., WANG Y.Y., WAN C.C., *Conductivity study of porous plasticized polymer electrolytes based on poly(vinylidene fluoride) – A comparison with polypropylene separators*, Journal of The Electrochemical Society **147**(9), 2000, pp. 3219–3225.
- [11] SAMAR KUMAR MEDDA, DEBTOSE KUNDU, GOUTAM DE, *Inorganic–organic hybrid coatings on polycarbonate: Spectroscopic studies on the simultaneous polymerizations of methacrylate and silica networks*, Journal of Non-Crystalline Solids **318**(1–2), 2003, pp. 149–156.
- [12] POINSIGNON C., *Polymer electrolytes*, Materials Science and Engineering: B **3**(1–2), 1989, pp. 31–37.

- [13] DAHMOUCHE K., SANTILLI C.V., DA SILVA M., RIBEIRO C.A., PULCINELLI S.H., CRAIEVICH A.F., *Silica-PEG hybrid electrolytes: structure and properties*, Journal of Non-Crystalline Solids **247**(1–3), 1999, pp. 108–113.
- [14] DE SOUZA P.H., BIANCHI R.F., DAHMOUCHE K., JUDEINSTEIN P., ROBERTO M. FARIA R.M., BONAGAMBA T.J., *Solid-state NMR, ionic conductivity, and thermal studies of lithium-doped siloxane–poly(propylene glycol) organic–inorganic nanocomposites*, Chemistry of Materials **13**(10), 2001, pp. 3685–3692.
- [15] YONG-IL PARK, MASAYUKI NAGAI, *Proton-conducting properties of inorganic-organic nanocomposites, proton-exchange nanocomposite membranes based on 3-glycidoxypropyltrimethoxysilane and tetraethylorthosilicate*, Journal of The Electrochemical Society **148**(6), 2001, pp. A616–A623.
- [16] HUNT A., *Statistical and percolation effects on ionic conduction in amorphous systems*, Journal of Non-Crystalline Solids **175**(1), 1994, pp. 59–70.
- [17] ŻELAZOWSKA E., ZIEMBA B., LACHMAN W., *Counter electrodes for WO₃-based electrochromic coatings*, Optica Applicata **30**(4), 2000, pp. 663–670.
- [18] BOONSTRA A.H., MEEUWSEN T.P.M., BAKEN J.M.E., ABEN G.V.A., *A two-step silica sol–gel process investigated with static and dynamic light-scattering measurements*, Journal of Non-Crystalline Solids **109**(2–3), 1989, pp. 153–163.
- [19] DOO-HYUN LEE, JIN-WOONG KIM, KYUNG-DO SUH, *Monodisperse micron-sized polymethylmethacrylate particles having a crosslinked network structure*, Journal of Materials Science **35**(24), 2000, pp. 6181–6188.
- [20] SHUXUE ZHOU, LIMIN WU, WEIDIAN SHEN, GUANGXIN GU, *Study on the morphology and tribological properties of acrylic based polyurethane/fumed silica composite coatings*, Journal of Materials Science **39**(5), 2004, pp. 1593–1600.
- [21] PRIMEAU N., VAUTEY C., LANGLET M., *The effect of thermal annealing on aerosol-gel deposited SiO₂ films: a FTIR deconvolution study*, Thin Solid Films **310**(1–2), 1997, pp. 47–56.
- [22] YING J.Y., BENZIGER J.B., NAVROTSKY A., *Structural evolution of alkoxide silica gels to glass: effect of catalyst pH*, Journal of the American Ceramic Society **76**(10), 1993, pp. 2571–2582.
- [23] GÜNZLER H., GREMLICH H.-U., *IR Spectroscopy: An Introduction*, Wiley-VCH Verlag GmbH, Weinheim, 2002, pp. 189–246.
- [24] PARASHAR V.K., RAMAN V., BAHL O.P., *Sol–gel preparation of silica gel monoliths*, Journal of Non-Crystalline Solids **201**(1–2), 1996, pp. 150–152.
- [25] MUNRO B., *Ion-conducting properties of SiO₂ gels containing lithium salt*, Glass Science and Technology – Glastechnische Berichte **68**(4), 1995, pp. 123–132.
- [26] KYOUNG-HEE LEE, KI-HO KIM, HONG S. LIM, *Studies on a new series of cross-linked polymer electrolytes for a lithium secondary battery*, Journal of The Electrochemical Society **148**(10), 2001, pp. A1148–A1152.
- [27] EISENBERG A., *Physical Properties of Polymers*, 2nd Ed., American Chemical Society, Washington DC, 1993, p. 88.
- [28] DONNADIEU A., *Electrochromic materials*, Materials Science and Engineering: B **3**(1–2), 1989, pp. 185–195.
- [29] ÖZER N., *Electrochemical properties of sol–gel deposited vanadium pentoxide films*, Thin Solid Films **305**(1–2), 1997, pp. 80–87.
- [30] COGAN S.F., NGUYEN N.M., PERROTTI S.J., RAUH R.D., *Optical properties of electrochromic vanadium pentoxide*, Journal of Applied Physics **66**(3), 1989, pp. 1333–1337.
- [31] ASHRIT P.V., BADER G., TRUONG V.V., *Electrochromic properties of nanocrystalline tungsten oxide thin films*, Thin Solid Films **320**(2), 1998, pp. 324–328.
- [32] COGAN S.F., PLANTE T.D., PARKER M.A., RAUH R.D., *Electrochromic solar attenuation in crystalline and amorphous Li_xWO₃*, Solar Energy Materials **14**(3–5), 1985, pp. 185–193.

Received November 12, 2009
in revised form January 4, 2010